Convergent-Beam Low Energy Electron Diffraction (CBLEED) and the Measurement of Surface Dipole Layers

J. C. H. Spence[1], H. C. Poon[2], D. K. Saldin[2]

[1]Dept. of Physics and Astronomy
Arizona State University
Tempe, Az. 85287-1504 USA

[2]Department of Physics and Laboratory for Surface Studies,
University of Wisconsin-Milwaukee,
Milwaukee, WI 53211 USA.

Abstract: We propose the formation of LEED patterns using a highly convergent beam forming a probe of nanometer dimensions. A reflection rocking curve may then be recorded in many diffraction orders simultaneously. Multiple scattering calculations show that the intensity variations within these rocking curves is as sensitive to the parameters describing the surface dipole layer as conventional I/V scans. However the data may be collected from areas sufficiently small to avoid defects and surface steps, radiation damage controlled by use of low voltages, and the information depth selected by choice of the (constant) voltage. We briefly discuss also the application of this method to oxides, and the formation of atomic-resolution scanning images in an idealized instrument in which coherent diffracted LEED orders overlap.

keywords: LEED, Convergent beam, Nanoprobe, Dipole layer

Paper for John Cowley's 80th birthday Festschrift
To be published in *Microscopy and Microanalysis*.

INTRODUCTION

The chemical reactivity of surfaces depends sensitively on the nature of the surface potential, and this, for an atomically smooth surface, is dominated by the surface dipole layer. (For stepped surfaces, the dipole is reduced by the Smoluchowski effect). The resulting potential controls a wide range of phenomena in surface chemistry, from catalysis to crystal growth. A variety of phenomenological models have been proposed for the form of this potential (e.g. (Jones, Jennings et al. 1984)), which also affects the magnitude of the mean value of the electrostatic inner potential (Saldin and Spence 1994). Dipole layers are present in metals and, to a greater extent, in ionic crystals (Peng, Dudarev et al. 1998), which we also discuss for the interesting case of the strongly-correlated transition metal oxides, frequently used as catalysts. The measurement of the surface potential has proven difficult, since few techniques exist for its measurement. (These include the measurement of secondary electron emission energy distributions and resonance effects in LEED (Venables 2002)). Two recent novel approaches include the use of resonance effects in RHEED for the ionic surfaces of strongly-correlated d-electron oxides (Peng, Zuo et al. 1998), and the use of a sub-nanometer probe in STEM (Tan and Cowley 1984). In addition, spot-splitting in RHEED at steps due to some rays entering a surface and emerging at a step face can be used to measure the mean inner potential (Yamamoto and Spence 1983; Peng, Zuo et al. 1998), which depends on the dipole layer. Physically, the dipole layer acts like a capacitor and hence an electrostatic beam deflector, pulling the RHEED pattern down with respect to the Kikuchi background (Peng, Zuo et al. 1998). Elastic energy-filtering has been applied to convergent-beam RHEED data for this purpose also (Ichimiya, Kambe et al. 1980) (Zuo, Weierstall et al. 2000) . Sensitivity to this potential requires a charged probe with low kinetic energy in the direction normal to the surface - this can be achieved in LEED at energies below about 20eV, or in RHEED at small glancing angles. Quantification of the data is complicated by intense multiple elastic scattering from an optical potential whose imaginary part has not been calculated accurately. Elastic energy-filtering is desirable.

At high energies in the transmission geometry, a minor revolution has occurred recently as, for the first time, it has become possible to very accurately quantify multiple-scattering electron diffraction data from thin crystals (Spence and Zuo 1992). This has come about for several reasons, including the availability of imaging energy filters, cooling stages, CCD detectors, and, above all, the use of the convergent-beam geometry. This geometry provides a very small probe (ensuring high crystal perfection for the region studied) while paradoxically giving more information about this region as the probe size is reduced. (For a diffraction-limited probe, the size of the angle-resolved cone of scattering generated for each Bragg order increases as the probe size is reduced). Thus, as in X-ray work, sample quality (e.g. mosaic block structure or surface defects) had previously limited accuracy, rather than experimental technique. The ability which a small probe provides in making extinction-free measurements of crystal structure factors then provides a sufficient increase in accuracy (to the 0.1% level) to allow direct "imaging" of chemical bonds in real materials (Zuo, Kim et al. 1999).

In this paper we consider whether these benefits of the convergent-beam geometry may be extended to low energies for the study of surface potentials. Rather than study I/V curves, in which the intensity of Bragg beams is studied as a function of their kinetic energy, we propose the use of a fixed energy, large illumination angular divergence, and a small focussed probe originating from a field-emission source. The intensity variation within the angular "rocking curve" of each beam is then used to model the surface potential. The use of a large illumination angle to produce a smaller focussed probe would then allow the study of submicron surface regions, whose freedom from defects might provide microdiffraction patterns of sufficiently high quality to justify accurate quantification.

THE CBLEED GEOMETRY

Figure 1 shows the geometry proposed for convergent-beam LEED (CBLEED). The incident beam is taken normal to a low-index surface plane. Provided that the illumination angle is less than the Bragg angle, a patch of intensity will be created around each LEED Bragg spot whose shape is approximately that of the illumination aperture, normally circular. Structure within this patch is sensitive to the surface potential, since, as shown in figure 1, for

each point in the incident cone, the elastically scattered beams explore different points along the rods in reciprocal space ("relrods"), whose form derives from the variation of potential normal to the surface. The incident cone may be decomposed into plane-wave components originating from points at infinity, each of which defines a set of conjugate points, one in each diffracted disk. (A single source *point* at infinity produces a single set of Bragg-related *points* in the scattering pattern if defects and inelastic scattering can be neglected). Inelastic scattering and diffuse elastic scattering from defects such as surface steps will produce a complicated convoluted pattern whose interpretation is difficult and depends on the coherence properties of the electron source. However the use of a very small field-emission probe facilitated by the CBLEED geometry, and elastic energy-filtering, will minimize these effects. In this paper we ignore inelastic scattering (apart from its depleting effect on elastic scattering) and defects.

MULTIPLE-SCATTERING CALCULATIONS FOR CBLEED FOR METALS

Convergent beam LEED calculations are performed by a standard LEED program (Van Hove and Tong 1979) assuming a model

$$V(z) = \frac{1-\exp[\lambda(z-z_o)]}{2(z-z_o)} \qquad for \quad z \le z_o$$

$$= \frac{-U_o}{A\exp[\beta(z-z_o)]+1} \qquad for \quad z \ge z_0$$

of the surface potential proposed by Jones et al. (1984), where $\beta = U_0/A$ and $A = -1+2U_o/\lambda$. The three adjustable parameters U_o , λ and z_o define the dipole layer potential by characterizing the barrier height, width and position (relative to the outermost plane of atoms in the crystal) of the image plane, respectively, as shown in figure 2. The electron scattering by this surface potential is calculated by the invariant imbedding R-matrix method proposed earlier by Zhao, Poon et al. (1988) for RHEED. This method converts the Schrödinger equation of the projectile electron into a nonlinear differential equation in R, which can be integrated into the crystal half-space from the surface. Reflection and transmission coefficients of the surface potential are then

obtained in terms of R, and combined with the reflection matrices of the ensemble of atomic layers of the crystal from a conventional LEED calculation by a layer stacking method (Pendry, 1974) to find the combined reflection matrix of the surface barrier and the atomic layers. The calculation of LEED I/V curves by this method have been reported previously for a Ag (111) film on a W(110) substrate (Poon, Tong et al. 1998). Effects of the electron exchange potential are included in the LEED calculations of the atomic layers by Slater's prescription (Slater 1967) as is usual in LEED (Pendry 1974). As for the model surface potential, it would normally incorporate exchange effects by fitting its adjustable parameters to experimental data. (In our present work these parameters are varied to test their effects on calculated convergent-beam LEED patterns). This calculation fully includes all elastic multiple scattering from the model of the surface potential and the atomic layers.

Initial calculations were made for Al(100) and W(100). In each case, for a circular illumination aperture, the beam divergence is the greatest possible consistent with non-overlapping orders of convergent-beam discs (i.e. the ones corresponding to neighboring Bragg beams just touch at their tangents). For a wide range of materials the minimum in the inelastic mean free path occurs around 50 eV (see e.g. Zangwill 1988), so that for energies below and above that, penetration increases. Figure 3 depicts calculated CBLEED patterns for Al(100) that span this energy. They show some structure within the CBLEED disks for energies either well above or below this minimum in the mean-free path. For the purpose of this demonstration, we have assumed a simple "no-reflection" step of -11.2 eV in the potential at the surface.

Figure 4 shows calculations for W(100) intended to indicate the sensitivity of these patterns to the parameters of Jones' model (Jones, Jennings et al. 1984) of the surface potential, given above. The beam energy is 4.6 eV, at which a prominent surface resonance is observed in experimental data from W(100). The barrier width λ takes the values 0.3 a_o^{-1} in panel (a), 0.8 a_o^{-1} in panel (b), and 1.3 a_o^{-1} in panel (c), where a_o is a Bohr radius (0.0529 nm). Other parameters, U_o = 1 Rydberg and z_o = -3.1 a_o are held constant in each case. Figure 5 shows this sensitivity more clearly with line traces of intensity against k_X across a "horizontal" line through the center of Figure 4. The boundaries of the diffracted orders are indicated. Figures 6 and 7 show similarly the sensitivity to the barrier position z_o with other parameters held constant, again for a beam energy of 4.6 eV and with U_o = 1 Rydberg and λ = 0.8 a_o^{-1}. From these line traces it is seen that

CBLEED is extremely sensitive to the details of the surface potential. From figures 6 and 7, we see that changes of a tenth of an Angstrom in the position of the barrier cause large, easily measured angular shifts in the position of the peaks in the rocking curves (figure 7). From figures 4 and 5, similar changes in the width of the barrier are seen to have a similar effect. By comparison with I/V curves, these data show similar sensitivity, but could be obtained from microdiffraction patterns from much smaller areas which are more likely to be free of the surface steps responsible for diffuse scattering. In addition, by obtaining all the data at one low energy, radiation damage effects may be minimized. LEED studies of organic materials (Firment and Somorjai 1979), in which the time for spots to fade is measured as a function of beam energy, show dramatic improvements at lower energies, where fewer states exist into which excitations can occur.

SCANNING IMAGING BY CBLEED.

Movement of the fine focussed probe in this arrangement allows a spatial map of the dipole layer to be formed, and regions free of defects also to be sought for analysis. In the future, the formation of a coherent probe whose dimensions are comparable with the dimensions of the unit cell may be possible. (The recent construction of aberration-corrected low voltage PEEM instruments in Berlin and Berkeley, aimed at about 2nm resolution, suggests that this may not be unrealistic). Then, by analogy with scanning transmission electron microscopy, it may also be possible to form images at near-atomic resolution by displaying a portion of the CBLEED pattern as a function of the focussed probe position. This portion should consist of the region in which the diffracted disks overlap, as discussed elsewhere in detail in connection with the theory of STEM lattice imaging (Spence and Cowley 1978) . The requirement that a diffraction limited coherent probe be formed whose width is less than that of the surface unit cell is equivalent to the condition that the coherent diffraction disks just overlap. Then the coherent interference between orders provides an imaging signal with the periodicity of the surface lattice, and a variety of optimized detector shapes can be considered. A large inelastic background, independent of probe position, can be expected. The information depth of this image will vary with accelerating voltage according to the universal curve discussed above, so that for energies well below or above the energy for minimum penetration, images of buried interfaces might be obtainable. Simulations for these imaging conditions are under way. The construction of a low-

voltage field emission electron gun for such an instrument is a highly challenging project, in view of the sensitivity of the probe to stray fields.

DISCUSSION AND CONCLUSIONS.

It is of interest to consider the extension of these results to dielectric materials. The results of calculations for the surface potential of an ionic oxide have been published previously (Peng, Dudarev et al. 1998). By comparison with metals, these show that a much larger dipole layer exists for this class of materials, which have important applications as catalysts. Similar large effects can be expected for most of the strongly correlated transition metal oxides, such as superconductors and colossal magnetoresistance materials. For these oxides, there are three cases : i) those in which ions are arranged in such a way that each plane parallel to the surface carries zero net charge. Then the projection of the dipole moment normal to the surface is zero. ii) those for which each atomic layer carries a net charge, but the repeat unit measured normal to the surface possesses zero dipole moment. iii) Other cases. For this third class of material, by extension of the results of the calculations reported here we expect a strong and measurable surface dipole layer to be detectable by CBLEED. As discussed in detail elsewhere, (O'Keeffe and Spence 1993), the choice of unit cell is not unique, and the dipole moment of a cell depends on this choice. However it will be found that different choices of cell result in different terminating layer structures which compensate for effects due to the choice of bulk cell, and the net dipole moment for an entire slab will then be found to be independent of the choice of cell. Experimental studies of these materials have been limited by sample charging effects, however these may be controlled by either doping or the use of thin films on a conducting substrate.

In summary, the multiple scattering calculations reported here suggest that the chemically important surface dipole layer might be mapped out by a new technique, convergent-beam LEED, in which LEED rocking curves are analyzed at a single energy using a fine probe. Radiation damage is minimized, a large amount of data is collected from a small, defect-free region, and, by scanning the probe, a spatial map of the dipole layer may be formed. We are currently modifying an experimental LEED apparatus for this purpose.

ACKNOWLEDGEMENTS

We are grateful to U.Weierstall, R. Tromp, and Q.Chen for useful discussions. Supported by ARO award DAAD190010500 (JCHS PI), DOE grant DE-FG02-84ER45076 and NSF grant DMR-9972958-001 (DKS PI).

References.

Firment, L. and Somorjai, G. (1979). Low energy electron diffraction studies of the surfaces of molecular crystals. Surface Science **84**: 275.

Ichimiya, A., Kambe, K. and Lehmpfuhl, G. (1980). Observation of the surface state resonance by the CBED RHEED technique. J. Phys. Soc. Jpn. **49**: 684.

Jones, R. O., Jennings, P. J. and Jepson, O. (1984). Surface barrier in metals: A new model with application to W(001). Phys Rev **B29**: 6474.

O'Keeffe, M. A. and Spence, J. C. H. (1993). On the average coulomb potential and constraints on the electron density in crystals. Acta Cryst. **A 50**: 33-45.

Pendry, J. B (1974). Low energy electron diffraction. Academic Press, London.

Peng, L. M., Dudarev, S. and Whelan, M. (1998). Electron scattering factors for ions and dynamical RHEED surfaces of ionic crystals. Phys Rev **B57**: 7259.

Peng, L. M., Zuo, J. M. and Spence, J. C. H. (1998). RHEED studies of the surfaces of ionic crystals. Int Congr. Electr. Micros., Cancun.

Poon, H. C., Tong, S. Y., Chung, W. and Altman, M. (1998). LEED analysis of Ag on W(110). Surf. Rev. Lett. **5**: 1143.

Saldin, D. and Spence, J. (1994). On the mean inner potential in high and low energy electron diffraction. Ultramicros. **55**: 397-406.

Slater, J. C. (1967). Insulators, Semiconductors and Metals. McGraw Hill, New York.

Spence, J. C. H. and Cowley, J. M. (1978). Lattice Imaging in STEM. Optik **50**: 129.

Spence, J. C. H. and Zuo, J. M. (1992).Electron Microdiffraction. Plenum, New York.

Tan, C. and Cowley, J. (1984). Surface potential study of Au(111). Ultramic **12**: 333.

Van Hove, M. A. and Tong, S. Y. (1979). Surface Crystallography by LEED. Springer-Verlag, Berlin.

Venables, J. (2002).Introduction to surface and thin film processes. Cambridge Univ. Press, N.Y.

Yamamoto, N. and Spence, J. C. H. (1983). Surface Imaging of Semiconductors by Reflection Electron Microscopy and Inner Potential Measurements. Thin Solid Films **104**: 43-55.

Zangwill, A. (1988) Physics at Surfaces. Cambridge Univ. Press, Cambridge.

Zhao, T. C., Poon, H. C. and Tong, S. Y. (1988). Invariant-embedding R-matrix scheme for reflection high-energy electron diffraction. Phys. Rev. **B38**: 1172.

Zuo, J. M., Kim, M., O'Keeffe, M. and Spence, J. C. H. (1999). Observation of d holes and Cu-Cu bonding in cuprite. Nature **401**: 49-52.

Zuo, J. M., Weierstall, U., Peng, L. M. and Spence, J. C. H. (2000). Surface sensitivity of CB-RHEED: Si (001) 2x1 models compared with dynamical simulations. Ultramic **81**: 235-244.

CAPTIONS.

Figure 1. CBLEED. Overlap of orders occurs if the illumination angle Θ becomes so large that $K_S(g)$ becomes parallel to $K_S(0)$. This occurs if the illumination divergence angle θ exceeds the Bragg angle.

Figure 2. Form of the surface barrier potential used in these simulations. Parameters are $U_0 = 1$ Rydberg , $\lambda = 0.8\ a_o^{-1}$, and $z_o = -3.1\ a_o$ (where a_o is a Bohr radius) corresponding to conditions used for figures 4b and 6b.

Figure 3. Dynamical convergent-beam LEED simulations for Al(100) at three energies, (a) 10 eV, (b) 50 eV and (c) 200 eV. The divergence of the incident beam is just sufficient for the convergent-beam discs associated with each Bragg order (some of which are indexed) to just touch. For the purposes of this demonstration, the surface is represented by a simple "no-reflection" step of -11.2 eV in the potential.

Figure 4. Dynamical convergent-beam LEED simulations for W(100) at 4.6 eV showing sensitivity to barrier width λ, which takes the values (a) $0.3\ a_o^{-1}$, (b), $0.8\ a_o^{-1}$, and (c) $1.3\ a_o^{-1}$. Here $U_o = 1$ Rydberg and $z_0 = -3.1\ a_o$ in each case. The beam divergence satisfied the same condition as that in Figure 3, but due to the low energy, only the specular convergent-beam disc is visible.

Figure 5. Line traces along k_x, from figure 4 taken horizontally through the center. λ takes the values of $0.3\ a_o$ (dashed line), $0.8\ a_o$ (solid line), and $1.3\ a_o$ (dots). U_o=1 Rydberg, and $z_o = -3.1\ a_o$ in each case.

Figure 6. Dynamical convergent-beam LEED simulations for W(100) at 4.6 eV showing sensitivity to the barrier position z_o, which takes the values (a) $-2.8\ a_o$, (b) $-3.1\ a_o$, and (c) $-3.4\ a_o$. Here $U_o = 1$ Rydberg and $\lambda = 0.8\ a_o^{-1}$ in each case. Beam divergence satisfies the same condition as that in Fig. 3, but due to the low energy, only the specular convergent-beam disc is visible.

Figure 7. Line traces along k_x, from figure 6 taken horizontally through the center. z_o takes the values -2.8 a_o (dashed line), -3.1 a_o (solid line), and -3.4 a_o (dots). Uo=1 Rydberg and λ=0.8 a_o^{-1} in each case.

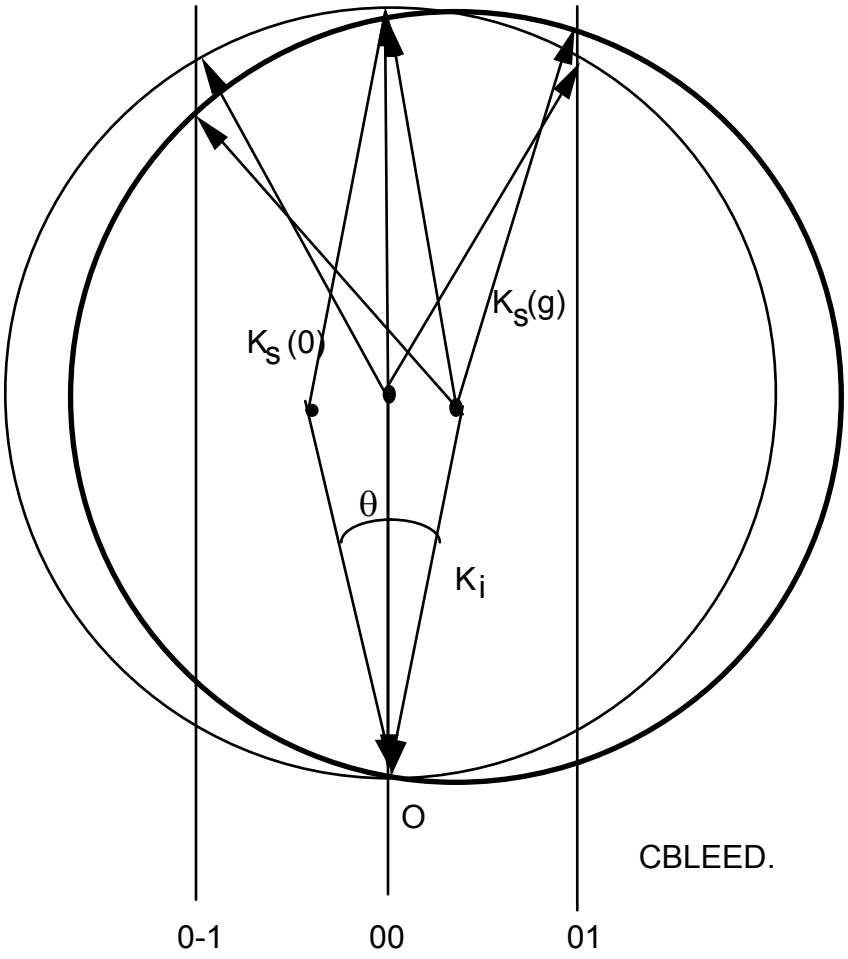

Figure 1.

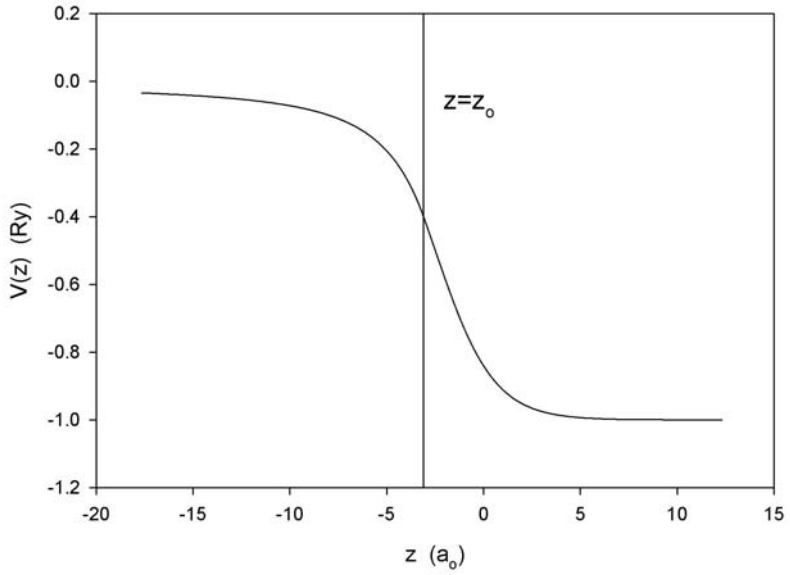

Figure 2.

(a)

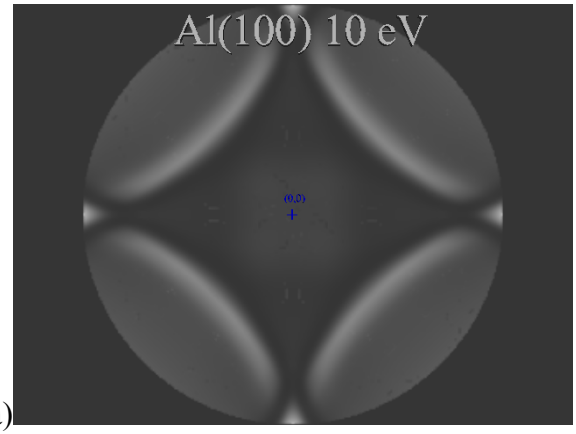

(b)

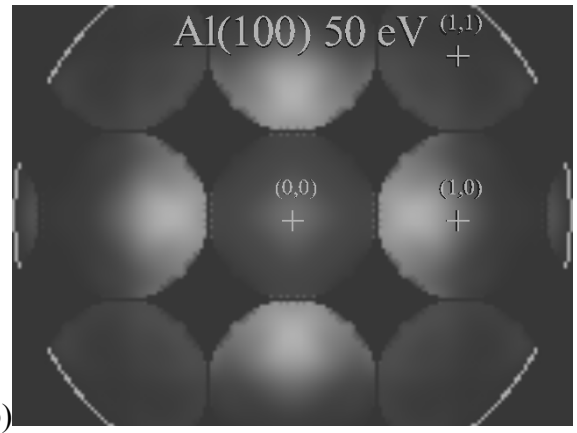

(c)

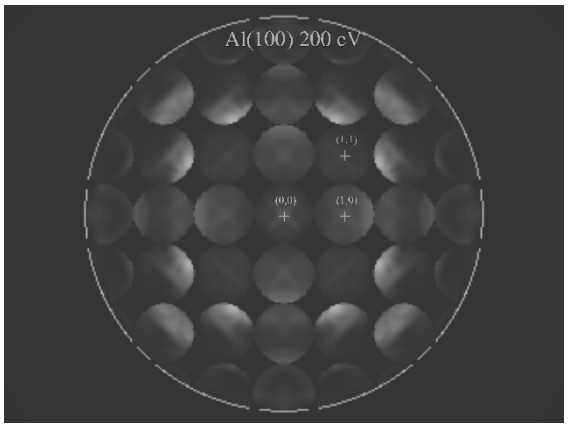

Figure 3.

(a)

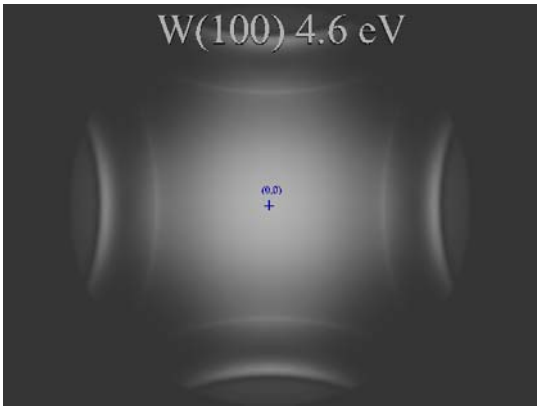

(b)

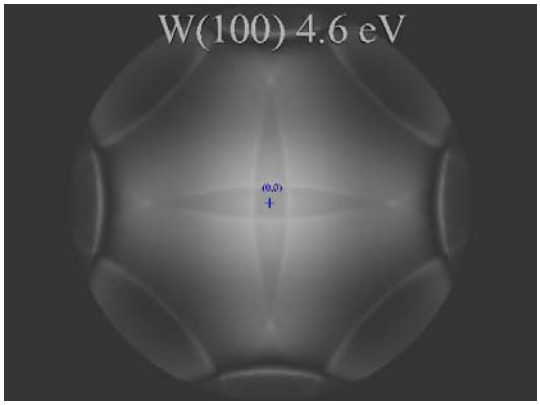

(c)

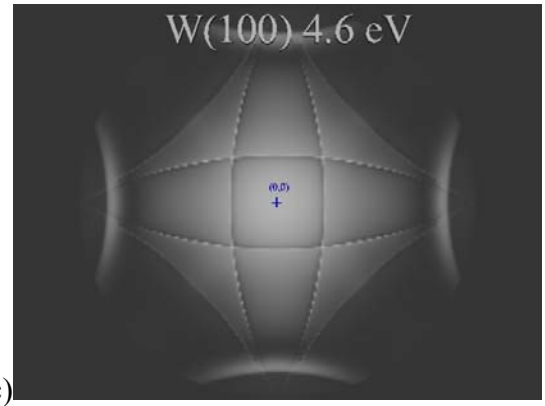

Figure 4.

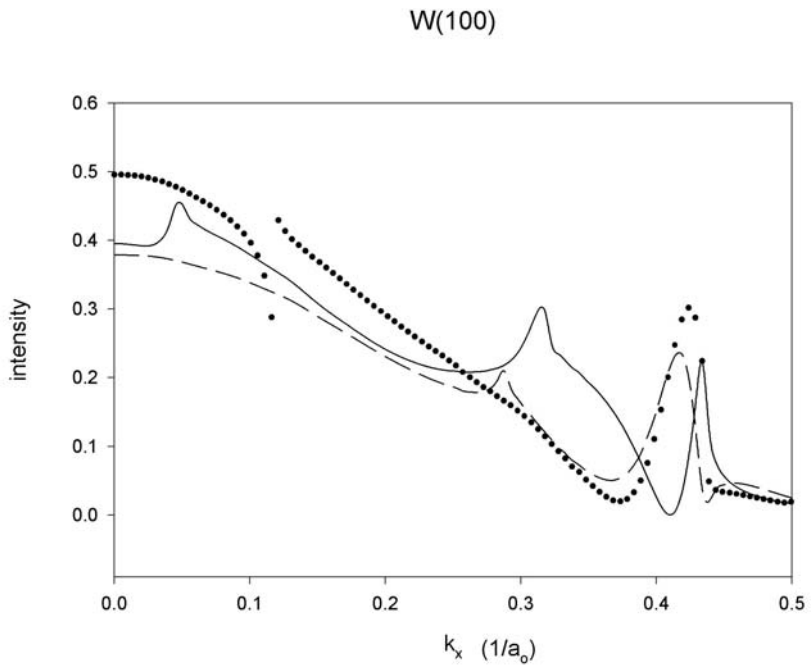

Figure 5.

(a)

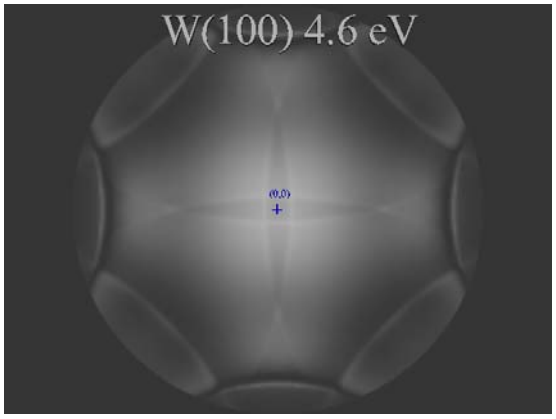

(b)

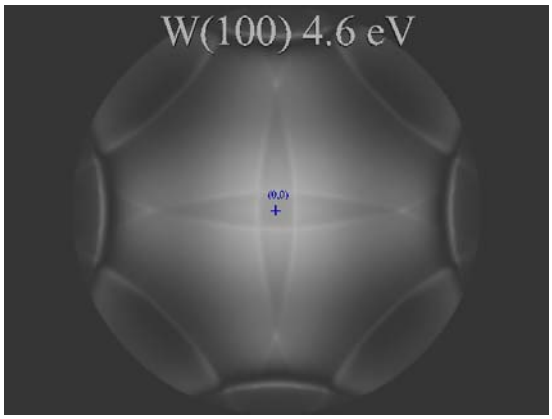

(c)

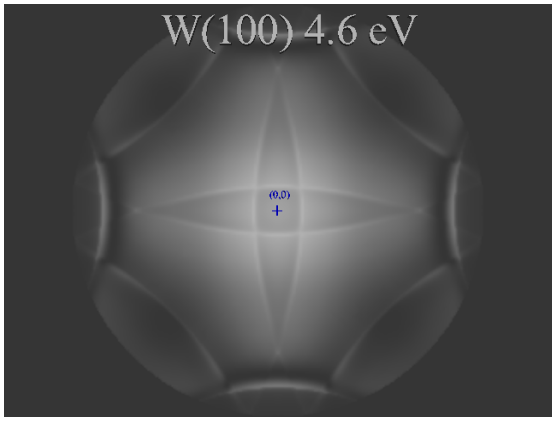

Figure 6.

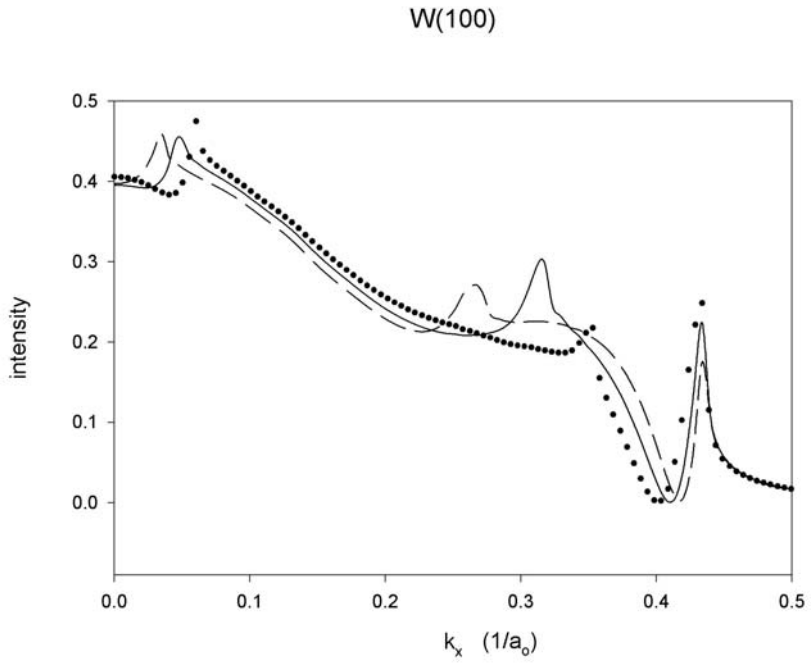

Figure 7.